International Journal of Digital Innovation in the Built Environment
Volume 11 • Issue 2

The Impacts of Early Architectural Design Decisions on Building Performance

Orçun Koral İşeri, Middle East Technical University, Turkey*
Onur Dursun, Liverpool John Moores University, UK

ABSTRACT

The early architectural design involves the most salient decisions. However, because of the large amount of variance, the decision-making is highly arduous. This article presents a methodology to enable the most effective design variables to be selected within the most effective value range by presenting a method that allows the measurement of output uncertainty depending on the impact of design decisions on outputs. The methodology was tested with different building functions and climate regions using two-phase sensitivity analysis. The values of design variables were generated with quasi-random sampling. They were sorted with factor prioritization. Ineffective variables were eliminated with factor fixing. Advanced global sensitivity analyses were performed for the total effect. Factor mapping was applied with the output weighting. The results were presented with parallel coordinate plot (PCP). The designers can make selections from alternatives with PCP. Finally, the study demonstrated how climate and building functions should be considered for building performance.

KEYWORDS

Early Architectural Design, Building Function, Cooling Energy, Decision-Making, Global Sensitivity Analysis, Heating Energy, Overheating Degrees, Performance-Based Design, Quantitative Analysis

INTRODUCTION

In recent years, the performance-based architectural design approach has become significant because of climate change impacts. The main causes of climate change are the increase in energy demand due to industrialization, the rapid growth of urban areas, and increased fossil fuel use (Mumovic, 2009). Thus, the design process needs to be energy efficient using analytical observations to apply better adaptation strategies against climate change. Although the building design and construction process involve many stakeholders, the most critical influence belongs to the architects. Although the designers are responsible for making important decisions regarding the building envelope and plan scheme (Granadeiro et al., 2013), many of them fall short of performance-based design and fail to grasp the process's advantages (Morbitzer, 2003). Due to the performance improvements requested or needed in architectural projects' proceeding stages, the design process's early stages are often

DOI: 10.4018/IJDIBE.301245 *Corresponding Author

returned. This situation causes losses of time and money (Hien et al., 2000). **Figure 1** points out that the most significant influence on buildings' energy performance comes from the early design process (Attia et al., 2012). For instance, improvements in the orientation of opening and building envelope design can reduce the building's energy demand by 40% (Wang et al., 2005). For this reason, the importance given to the early design stages should be increased by doing technical reviews to understand better the relationship between design decisions and building performance, e.g., building energy simulations, statistical data review.

The performance-based architectural design allows the designer to achieve better energy use and environmental performance. Because the designer can quantify and visualize the building performance. As an example methodology for performance-based design, genetic optimization algorithms are frequently used among designers (Kampf & Robinson, 2010; Konis et al., 2016). The optimization process leads to creating high-performance design solutions by automating the design process. In the process, the designer only edits the value ranges and constraints of the design variables. Nevertheless, the designer gains a limited understanding of the established design solution's reasons because of point-based performance estimation. Therefore, this approach falls short of meaningful evaluation of alternatives in early architectural design. An excellent solution to this problem can be found in statistical sampling methods to analyze the process's uncertainty and provide a powerful alternative to quantifying the relationship between design variables and performance outputs (Hemsath & Alagheband Bandhosseini, 2015).

This study uses the simulation-based methodology in a statistical analysis framework for an early architectural design feedback methodology by reaching quantitative results of building performance results. The building energy simulations are practical for more realistic decision-making (Morbitzer, 2003). However, energy simulations should be proactive for giving feedback about design variations (Attia et al., 2012; Kanters & Horvat, 2012; Rights, 2016). Unfortunately, most energy simulation tools cannot investigate the relationship between building and design variables in a proactive way (Y. Yildiz et al., 2012). Therefore, in this study, the authors suggest using statistical sensitivity analysis for proactive analysis. A systematic literature review was conducted of studies that statistical sensitivity analysis was proposed as an answer by measuring the output uncertainty and demonstrated the impact (i.e., effect) of the design variables (i.e., independent variable) on the performance outputs (i.e., dependent variable) for unbiased decision-making (De Wit & Augenbroe, 2002; O'Neill & Niu, 2017; Østergård et al., 2015; Ruiz Flores et al., 2012). Consequently, designers could have the possibility to reach effective design variable selection using performance output results.

The uncertainty analysis is an important issue for the early design decision-making process (Macdonald, 2002). Thus, Sensitivity Analysis (*SA*) is a valuable option to quantify the non-linear relationship between design variables and performance outputs. The framework is capable of in-depth exploration of the model attitude by scanning for all inputs' variations to measure each variable's influence on defined model performance output(s) (Firth et al., 2010; Iooss & Lemaître, 2015). Previous studies have shown that different *SA* methods are applicable to compute uncertainty of

Figure 1. Representation for the relationship between the effectiveness of the decisions and the lifetime of the building

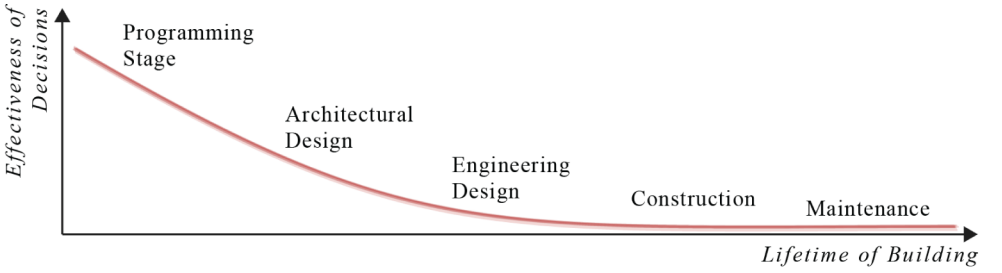

the dependent variables, i.e., screening inputs (Alam et al., 2004), meta-modeling by reducing the complexity of the energy model (Topcu & Ulengin, 2004), robustness framework (Burhenne et al., 2011).

SA is capable of identifying a-priori influence and rank the sensitivity of the independent variables. It is possible to investigate the 'What-if' question by measuring the individual and total impact (Struck et al., 2009). Thus, the technique is commonly used among designers (Kristensen & Petersen, 2016; Sun, 2015). SA methods are classified into two ways, i.e., local sensitivity analysis (*LSA*) and global sensitivity analysis (*GSA*) (Hemsath & Alagheband Bandhosseini, 2015). *LSA* performs better for the detection of the uncertainty of the input variables around a specified point. However, it is inefficient to quantify the interaction between independent variables (i.e., total effect). A considerable amount of literature has been published on *LSA* implementation on build energy modeling (Rasouli et al., 2013). *GSA* could scan the whole input set in terms of dependent variable activity, which contains an explanation for individual impact and total effect (Saltelli et al., 2007). The methodology frequently is used for early design building energy models, which score the total effect of independent variables (Menberg et al., 2016). Unlike *LSA*, all selected input variables are analyzed simultaneously in the statistical analysis process (Kristensen & Petersen, 2016). A large volume of published studies describe *GSA*'s role in building energy performance analysis (Østergård et al., 2017; Ruiz Flores et al., 2012; Yang et al., 2016), i.e., second-order quantification, factor mapping.

The design variable selections are essential for the early design process, and the proceeding design process follows these initial decisions. Therefore, early architectural design decisions should be analyzed to increase building performance. For various studies, analyses were rendered to quantify the design variables' impact for the different performance outputs at the initial architectural design steps (Depecker et al., 2001; Østergård et al., 2017). Thus, this study proposes a genuine model using *SA* by quantifying the impact of the design variables into the three-phases methodology for effective performance-based design decision-making process; (1) measuring the individual impact of design variables and fixing the ineffective design variables, (2) calculating the total effect of most effective design variables on the performance outputs, (3) robust mapping and visualization method for most effective design variables and performance output values in the aspect of interactive decision-making during early architectural design. If designers can instantly observe the effects of building design variables on performance outputs, buildings' energy use can be reduced much easier, and this can significantly contribute to adaptation strategies within the scope of climate change.

METHODOLOGY

The current study focuses on the early architectural design decision-making process to analyze design variables' impact on the performance outputs using a three-phase methodology (**Figure 2**). The proposed methodology has been tested with four case studies in terms of different building functions and climatic zones. The first two case study includes examining a residential unit in Istanbul and Izmir cities within the scope of sensitivity analysis based on the heating and cooling energy demand (*kWh/m^2-year*). The second two case study involves testing an office unit in Ankara and Kars' cities with sensitivity analysis according to heating energy demand and overheating degrees.

Model Description and Thermal Modeling

The analysis geometry, which is used for all case studies, is a hypothetical single-zone unit and the dimensions are *8 meters * 8 meters * 3 meters*. The total area and volume do not change during alternative generations. Except for the window-to-wall ratio and horizontal shading design variables, all design variables are construction-based or operational. In **Figure 3**, all design variables were explained with graphical visualization of where or what they effect the analysis geometry.

In this study, the performance outputs (i.e., dependent variables) are heating and cooling energy demand for the residential unit and heating demand and overheating degrees (*OHD*) for the office

Figure 2. Flowchart of the proposed model

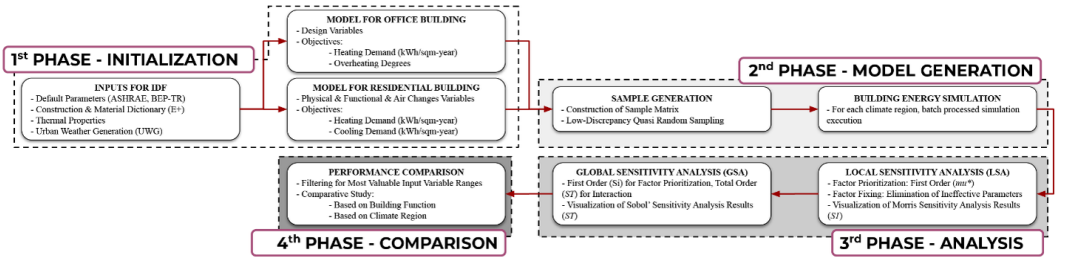

Figure 3. Digital building model initial dimensions with design variables

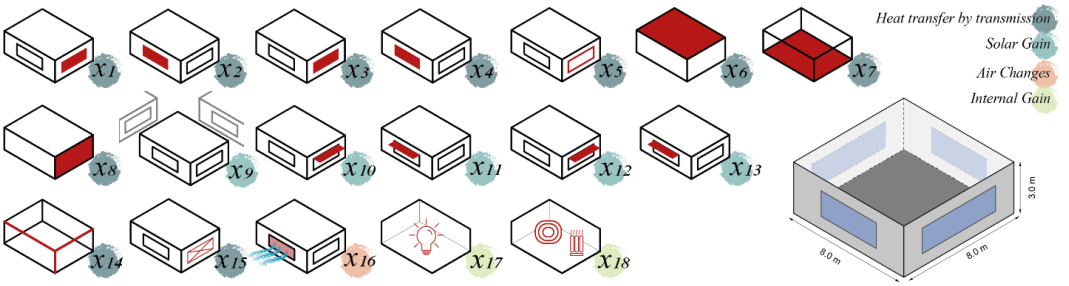

unit. The heating and cooling demand were annually calculated per sqm. *OHD* was calculated using a fixed upper-temperature limit for each zone type. The calculation of *OHD* is the annual summation of the indoor operative temperature above 28°C for the living room and 26°C in the bedroom (CIBSE, 2006). The design variables (i.e., independent variables) were separated into four different groups (**Table 1**), i.e., heat transmission by conduction, solar gain, air changes, and internal gain. The values of design variables for generated alternatives were arranged as functions to modify the input data file (*.idf*) of the building energy simulation engine of the *EnergyPlus* (*E+*) (Winkelmann, 2000). The *EnergyPlus* input data dictionary (*.idd*) was taken as default for a thermo-physical function library. The other thermal properties of the energy model were selected according to (ASHRAE, 2004, 2013b).

The construction material organization consists of basic *EnergyPlus* definitions, e.g., thickness, thermal resistance, and thermal mass features. The two-layer constructions were defined for the surfaces of the digital building envelope. The symbols before the material name identify the material type and the constructions' layer (**Table 2**). *NoMass* materials are responsible for varying thermal transmittance of the *u*-value (kWh/m^2-K) of the construction variables. The material does not have any thermo-physical properties in terms of conductivity, density. For each surface, different *NoMass* materials were assigned.

The setpoint temperatures were different for two different climate type, i.e., warm-humid climate for the residential unit, cold-dry environment for the office unit. Setpoint temperatures refer to values under which degree heating should be activated or above the degree cooling should be activated; thus, the pre-defined values directly influence energy demand and indoor thermal comfort (I. Yildiz & Sosaoglu, 2007). For all regions, the setpoint temperature of heating is 22.0 °C, and the setback is 10 °C. For Istanbul and Izmir, the setpoint temperature of cooling is 26.0 °C and the setback is 28.0 °C.

The building energy model alternatives were generated with *Monte Carlo simulation* techniques, quasi-random sampling. Then, alternatives were simulated in *EnergyPlus* building energy simulation software (Reference & Calculations, 2015). *EnergyPlus* works with text-based file mode (*.idf*). In the proposed methodology, *.idf* was modified to implement thermal and geometrical design variable

Table 1. Design variables and performance outputs of the residential and office unit

Type	Physical	Physical	Physical	Physical	Physical	Physical	Physical	Physical	Physical
Decision Variable	WWR North (x_1)	WWR East (x_2)	WWR South (x_3)	WWR West (x_4)	U-value of the Window (x_5)	U-Value of Roof (x_6)	U-Value of Floor (x_7)	U-Value of Wall (x_8)	Context Height (x_9)
Range	[0.1-1.0]	[0.1-1.0]	[0.1-1.0]	[0.1-1.0]	[0.773-5.778] ** *W/m2-K*	[0.104-0.840] ** *W/m2-K*	[0.104-0.840] ** *W/m2-K*	[0.114-2.330] *W/m2-K*	[3-12] *meter*
Type	Physical	Physical	Physical	Physical	Physical	Physical	Functional	Functional	Functional
Decision Variable	SHD North (x_{10})	SHD East (x_{11})	SHD South (x_{12})	SHD West (x_{13})	Infiltration (x_{14}) ****	SHGC (x_{15})	Glazing Opening ***** (x_{16})	Lighting Density (x_{17})	Equipment Load (x_{18})
Range	[0.1-1.0]	[0.1-1.0]	[0.1-1.0]	[0.1-1.0]	[0.0001-0.0006] m^3/s *per* m^2	[0.132-0.905] **	[0.0-1.0]	[3-15] W/m^2	[3-15] W/m^2
PO	Heating Demand (kWh/m^2)			Cooling Demand (kWh/m^2) ***			Overheating Hours		

*Heat transfer by transmission: HTT, Solar Gain: SG, Internal Gain: IG, Air Changes: AC, WWR: Window-to-Wall-Ratio, SHD: Shading Depth, SHGC: Solar Heat Gain Coefficient

**Range values according to EnergyPlus Standard Constructions (LBNL, 2009)

***Cooling Demand is active only for Izmir (ASHRAE 3A) and Istanbul (ASHRAE 4A)

****ASHRAE.90.1.2013, ASHRAE.62.1.2013 (ASHRAE, 2013a, 2013b)

*****Glazing opening ratio for natural ventilation

Table 2. The properties of construction materials

Construction	Outside Layer	Layer 2	Layer 3	Initial U-value	Range of U-value*
Roof Construction	*M14a* 100mm heavyweight concrete	-	Material: No Mass: Roof	0.052	[0.052-0.752]
Exterior Wall Construction	*M01* 100mm brick	-	Material: No Mass: Wall	0.114	[0.114-2.330]
Floor Construction	*F16* Acoustic tile	-	Material: No Mass: Floor	0.318	[0.318-2.330]
Window Construction	*Sgl Clr 3mm*	*Clear 3mm*	Material:No Mass: Glazing	0.773	[0.773-5.778]

*Upper limit of constructions are the construction values of Energyplus construction library, i.e., ASHRAE_HOF_Materials

alternatives in the energy model. The *.idf* modification was realized for thermal and geometrical design variables using *eppy* and *Python 3.7* libraries (Philip et al., 2011). For sensitivity analysis calculation functions, the *SALib* library was chosen (Herman, J. & Usher, 2017). For each climate region, many simulations were needed to quantify the design variables' impact. Therefore, in this article, all process was coded as automated serial simulations with batch-processing (Python Software Foundation, 2020).

The conditioning system's set point and set back values are the identical for all case studies (**Table 3**). The glass opening ratio (x_{16}), is directly related to natural ventilation, so the conditions

Table 3. Thermal properties of building energy model for hypothetical units

Name	Heating Set Point/ Set Back	Cooling Set Point* /SetBack	Natural Ventilation	Ventilation Limits for Indoor	Ventilation Limits for Outdoor	Schedule for office **	Schedule for residential **
Value /Type	25.0,20.0	25.0, 100.0	Natural, one-sided	21.0, 24.0	17.0, 28.0	Small Building Office Occupancy	Midrise Apartment Occupancy
Unit	*°C*	*°C*	-	*°C*	*°C*	-	

*Cooling SetPoint is active only for Izmir (ASHRAE 3A) and Istanbul (ASHRAE 4A)
**EnergyPlus standard schedule library

and times of natural ventilation are arranged by air conditioning systems. Limits have been added to indoor and outdoor air temperatures to prevent any conflict between natural ventilation and air conditioning systems during the day. Otherwise, this may result in excessive energy use. Daily natural ventilation and air conditioning usage schedules were determined by default schedules selected from the *E+* library. Limit values for both examinations were determined according to ASHRAE standards (ASHRAE, 2013a).

Weather Data Selection and Urban Weather Data Generation

In this study, the simulations were produced in two building types and four different locations to compare climate and building function difference impact on the performance outputs. Residential unit simulations were executed for Istanbul and Izmir region, and office building simulations were in Ankara and Kars. Four different climate regions were grouped under two climate types. Istanbul (*ASHRAE climate zone 4A*, *Cooling Degree Days* 10°C £ 2500, *Heating Degree Days* 18°C £ 3000) and Izmir (*ASHRAE climate zone 3A*, 2500 < *Cooling Degree Days* 10°C < 3500) have warm-humid climate. Ankara (*ASHRAE climate zone 5B*, 3000 £ *Heating Degree Days* 10°C £ 4000) and Kars (*ASHRAE climate zone 7*, 5000 < *Heating Degree Days* 18°C £ 7000) have cold-dry climate.

Figure 4 represents the annual outdoor dry bulb temperature values comparison between selected climate regions. In this study, simulations were generated with annual weather data. On the other hand, simulations can be performed with a choice of two extreme weeks or different analysis periods to reduce the simulations' calculation costs. However, the simulations' accuracy is lower with other analysis period selections instead of using the annual simulation period.

The selected neighborhoods are in the center of urban; for this reason, building energy simulations were modified according to the urban heat island effect (e.g., atmospheric heat transfer from the urban canopy, building density, the reflection of solar radiation from facades). In general, the meteorological

Figure 4. Weather data comparison (ASHRAE, 2009)

stations' location is outside the city, thus, the effects of city elements are not sufficiently included in the weather data. The urban heat island effect modifications were executed using an urban weather data generation algorithm (Unzeta, 2010). The transformation tool is *Grasshopper/Ladybug* plugins based on *EnergyPlus* simulation software (Roudsari & Pak, 2013; Winkelmann, 2000). **Figure 5** points out the locations of the hypothetical units in the urban regions. These locations' environments were digitally modeled to implement urban features in the weather data. The chosen neighborhoods for Istanbul and Izmir consist of mostly residential buildings. For Ankara and Kars, mixed building function locations were selected.

Data Generation and Sampling

Monte Carlo simulation techniques work based on pseudo-random sampling methodology with a low discrepancy to visualize the multivariate global design space (**Figure 6-a**). In this workflow, input distributions and sampling strategies are first defined. Then, simulations are performed to determine performance outcomes. The methodology provides a global screening approach for performance output variance to complement the lack of comprehensive interpretation of point prediction-based systems or traditional non-performance-based methods. For this reason, it is prevalent in the field of building energy modeling (Haarhoff & Mathews, 2006).

The design variables' ranges are set as continuous [0-1] range values and are arranged as a uniform distribution. The discrepancy of the variable shows the global design space, which represents the variation of performance outputs. Therefore, the sampling technique provides independent variable sampling in terms of the probability distribution. The established variable ranges were interpreted as central 95% *confidence intervals*. As a result, as quasi-random sampling strategy leads to analyze all the

Figure 5. Urban simulation environments for each climate region

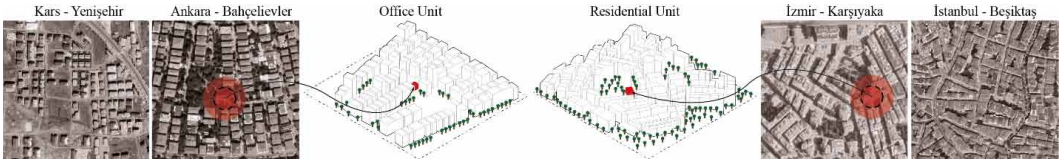

Figure 6. (a) Sampling Types; (b) Demonstration of the four-level grid, the arrows identify the eight points needed to estimate the elementary effects relative to factor X_1

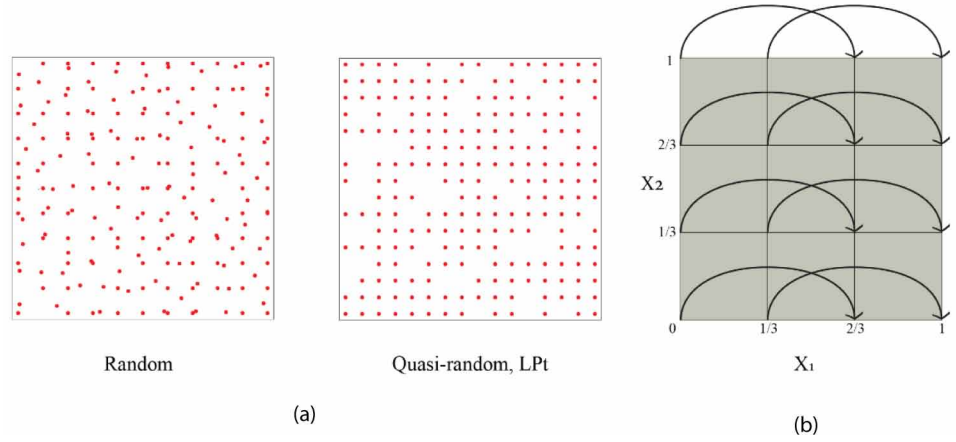

global design space, the method provides highly dependable results on how design variables interact with each other, and which variable range drives the most valuable results for performance outputs.

Local and Global Sensitivity Analysis

The building energy demand comprises multiple design variables, e.g., building envelope design, building energy system design and efficiency, the operational building systems, occupant density and activities, and finally, indoor air and environment quality measurement. All the design variables distinguish from each other in terms of their impact on different performance criteria. Global sensitivity analysis has a considerable role in determining the inputs' relative importance by analyzing the input variables' total influence and individual impact. Simultaneously, they all change by a basic sampling rule (Ruiz Flores et al., 2012). Hence, the holistic analysis can improve the performance of the building by observing all variables. The sensitivity analysis of the study has been divided into two phases in terms of methodological attitude. Firstly, *Morris* sensitivity analysis has applied depends on the degradation of the individual factor variance. Secondly, *Sobol*'s sensitivity analysis was rendered to disaggregate the inputs' total variance and individual change.

Morris sensitivity analysis is the screening method that visualizes the performance of the variable individual impact. It reduces the size of the model by removing the ineffective independent variables according to the order of the variables. *Morris* sensitivity analysis has been realized with the *Elementary-Effect* (*EE*) method (**Figure 6-b**), the variables' finite distribution. The analysis generates a large sample values for independent variables to determine which variable is ineffective for the dependent variable. It is suitable to show linear relations (Waqas et al., 2017). The main idea is to create *r* different trajectories in the *N*-dimensional design space (**Figure 6-b**). The N-dimensional variable space was normalized to [0,1] and was divided into *p*-levels by distinguished *p*-quantiles. Each trajectory includes *N + 1* calculations for a reason one-parameter-changes (*OAT*) by defined equal steps at a time. Thus, each variable relates to the *EE* by determining the model output variation at *r* different values. Input factor of *EE* (2) is represented with the mathematical equation as follows (Saltelli et al., 2007):

$$EE_i = \frac{\left[Y\left(X_1, X_2, ..., X_{i-1}, X_i + \Delta, ..., X_N - Y\left(X_1, X_2, ...X_N\right)\right)\right]}{\Delta} \tag{1}$$

where $\Delta \in \left[1/\left(p-1\right), \cdots, 1-1/\left(p-1\right)\right]$. Variable distributions were produced globally, which discretized the input area by the trajectories. When the value of variable changes, in the background, *Morris* sensitivity measures the absolute mean value (μ^*) and standard deviation (σ^2) of the distributions as (2,3):

$$\mu^* = \frac{1}{r}\sum_{j=1}^{r}\left|EE_i^j\right| \tag{2}$$

$$\sigma^2 = \frac{1}{r}\sum_{j=1}^{r}\left(EE_i^j\right)^2 \tag{3}$$

wherein both equations *r* represents the number of samples. The absolute mean value (μ^*) points out the total influence of variable (X_i) on the model output (Y). If μ^* of input is high, the variable has an essential impact on the output, which is not negligible. If σ^2 has a bigger value than the mean,

consequently, the computation of *EE* is positively impacted by the sample point. It means the variable based on the values of other inputs or the input has a non-linear relation with the specified output. However, the *Morris* sensitivity analysis is a local sensitivity analysis method. Therefore, the technique has capacity to state the non-linear relations of variables, but it could be insufficient to evaluate.

The initial phase is the extension of the qualitative presentation of the analyzing values. It is special to quantify the total output variance for each variable. The current method supplies a valid scale for determining which variable or variables are inefficient to define model output variance. On the other hand, by identifying the most influential variables on the performance output, it is possible the deduce output variance with the quantized technique (Rights, 2016).

Secondly, *Sobol* sensitivity analysis applied in which is one of the variance-based methods. Sobol sensitivity analysis has been performed with *Sobol* sequences low discrepancy method to screen the global design space. Its computing cost is more than *Morris* sensitivity analysis. It quantifies the individual variable influence (i.e., first-order) on the model output, interactions between variables (i.e., second-order), and total impact for the model outputs. A pseudo-random sampling of *k*-dimensional points has a high discrepancy. However, there are infinite sequences of *k*-dimensional points that act much confident concerning this measure. As the dimension length *N* increases, it can reduce the optimum ratio's inconsistency as a specification. As a result, an estimated mean for a function $Y\left(X_1, X_2, X_3, \cdots, X_k\right)$ was evaluated on points $\left\{X_{i1}, \cdots, X_{ik}\right\}_{i=1,N}$. Such a sequence can bring the inconsistency closer to optimal levels by finding the predicted average faster than the predicted mean of randomly generated points.

The *Sobol sequence sampling* returns a matrix that includes model input values. The pre-defined *Saltelli sampling* was preferred, which is the basic extension of *Sobol sequence* (Saltelli et al., 2007). For each sampling strategy, concerning procedure $N \times \left(D + 2\right)$ times, rows are produced in which *N* is the number of samples to generate, and *D* is the number of independent variables. Besides, if second-order calculation is implicated in the process, which is the value defining the total influence of all input variables on the output, the equation is converted $N \times \left(2D + 2\right),$ and it is seen to computing cost increases. In this study, second-order calculations were realized in the second step of the proposed methodology for the interaction quantification of the variables.

Method of *Sobol* is suitable when the model is non-linear, and *Sobol* indices can explain the decomposition of the output. Sobol sensitivity analysis has three indices that analyze the input conduction (Iooss & Lemaître, 2015). First-order (S_i), the main effect of the index separately for each variable without interactions, the higher value of S_i, the more significant the influence on the i^{th} factor for the output variance. The second-order index measures the contribution of the output variance by the interaction of two model inputs. Total order (i.e., Total-effect) (S_T), this index measures the contribution to X_i's output variance, including all variance caused by its interactions, of any order, with any other input variables.

The variance-based model function is $Y = f(X)$ where Y is the output and $Y = (x_1, x_2, \ldots\ldots x_k)$ are *k*-independent points that each variable changes by their probability density as the *Sobol* demonstrate (Sobol, 2001), any square-integrable mathematical function can be solved by a unique figuration of the high dimensional model (4) when the input variables are independent of each other:

$$V_y = \sum_{i=1}^{k} V_i + \sum_{i>j}^{k} V_{ij} + \cdots + V_{12\cdots k} \tag{4}$$

V_y is the total variance of the performance outputs, and V_i is the residual variance produced by X_i and $V_{i1\ldots.is}$ and is to define collaborative fractional variance induced by $\{X_{i1\ldots\ldots}X_{is}\}$. Therefore (5):

$$\sum_{i=1}^{k} S_i + \sum_{i>j}^{k} S_{ij} + \cdots + S_{12\cdots k} = 1 \tag{5}$$

$Si = V_i / V_y$ is the first order index about sensitivity that calculates Y-induced variance by X_i. $S_{ij} = V_{ij} / V_y$ is the second-order index that calculates Y's variance by the interaction of two input variables, i.e., X_i and X_j. For all the individual variances and interactions were scaled into [0, 1] and all equal to 1. While the measurements of the sensitivity indices are in the linear relation with the number of inputs (i.e., 2^{k-1}), the computing cost of the calculation increases; therefore, in many cases, first-order (S_i) and total order (S_T) of the sensitivity indices are summarized in the one formula as follows (6):

$$S_{Ti} = S_i + \sum_{i \neq j}^{k} S_{ij} + \cdots + S_{12\cdots k} \tag{6}$$

The total sensitivity index includes all the X_i contributions (i.e., residual and collaborative) to Y's variance; thus, when its value is close to zero, X_i can be determined as non-significant. For this reason, the input factor can be counted as a default value by implementing factor fixing.

Factor Mapping and Output Score Weighting

Factor Mapping (*FM*) determines the values of variables that lead to model most realization in a given range of output space (Torben Østergård, 2017). For instance, one may want to highlight model realizations falling above the 95th percentile. Besides, the factor mapping is the extension of a sensitivity analysis to support how variable and variable range can provide a valuable solution due to the problem's definition. In this study, 100 best values are filtered for *Parallel Coordinate Plot* (*PCP*) from the vast global design cluster after *Sobol*'s variance-based analysis. Best performance values have corresponded to low energy demand in terms of two output variables for each region:

0.5 × (heating demand + cooling demand) = weighting score
0.5 × (normalized heating demand + normalized cooling demand) = weighting score

In this study, the best performances based on the performance outputs were sorted with the design variables that generate these performance results. The heating and cooling (*kWh/m²-year*) demand were outputs for Istanbul and Izmir. Performance outputs were unified with the linear calculation by forming the total energy demand (*kWh/m²-year*) as a single score function (1). The heating demand (*kWh/m²-year*) and overheating degrees were output for Ankara and Kars. Two outputs have different units and ranges; to calculate a weighting value, they were normalized between 0 to 1. Then, similar linear calculations (2) were applied for these output variables. This modification was be advantageous to decrease the computing-cost for process of the sensitivity analysis and give quick results, and the holistic score approach facilitates comparison when seizing on large numbers of design options (Østergård et al., 2015). Furthermore, it supports the rendition of sensitivity analysis and provides more salient filtering for quasi-random sampling. However, this unified linear calculation was only used for factor mapping.

RESULTS AND DISCUSSION

In this chapter, two process sensitivity analyses and performance filtering processes results were explained. 21000 simulations for *Morris* sensitivity analysis and 42000 simulations for the *Sobol* sensitivity analysis have been generated. Simulations include 18 different design variables (**Table**

1). Lastly, *PCP* were prepared to present all design variables and outputs in one chart and provide opportunity detail analyzes with brushing techniques. It is the visual explanation of the proposed methodology, which could help the designers during the early architectural design process.

Factor Prioritization and Factor Fixing

In the first phase of the proposed methodology, the *Morris* was applied to quantify the individual impact of 18 design variables on the performance outputs; then, the ineffective design variables were fixed. All design variables were calculated and presented on the horizontal bar and polar plot regarding their influence (*mu**) on the output (**Figure 7**, **Figure 8**). Eight variables for Istanbul and Izmir, nine for Ankara, and ten design variables were influential for two performance outputs. In this step, sensitivity analyzes were calculated separately for each output. If a design variable similarly has significant influence for two outputs, it was defined as effective and was transferred to the second step for global sensitivity analysis.

Sensitivity analysis for Istanbul and Izmir has resulted in analogous design variables (**Figure 7**). x_2, x_3, x_4, x_5, x_6, x_9, x_{14}, x_{15} were effective for the variance of the model's two outputs. Their influence values were also close to each other, and the small number of differences resulted from the climate differences. The climatic types of the two regions differ from each other in terms of humidity and outdoor temperature. Izmir region has higher values for both rates. x_2, x_3, x_4 are window-to-wall ratio (*wwr*) variables, x_{15} is the solar heat gain coefficient of the window construction, and x_9 is the height of the contextual buildings. These variables are directly related to the sunlight, which affects the daily

Figure 7. (a) Design variable influence on the horizontal bar chart for Istanbul and Izmir; (b) Comparison of most effective design variables between Istanbul and Izmir on Polar Chart

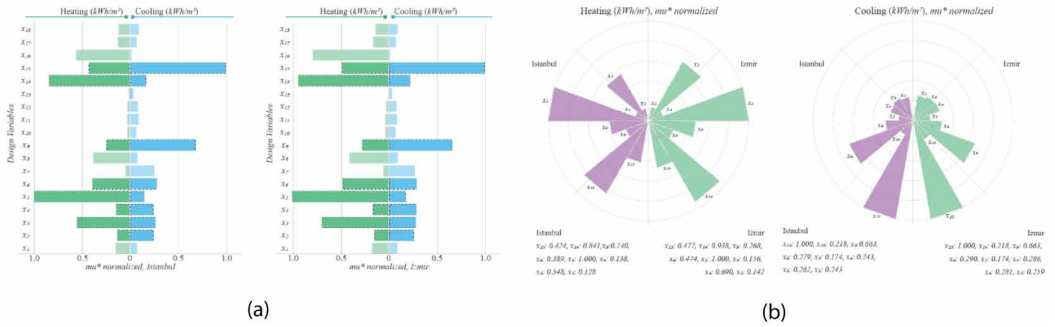

Figure 8. (a) Design variable influence on the horizontal bar chart for Ankara and Kars; (b) Comparison of most effective design variables between Ankara and Kars on Polar Chart

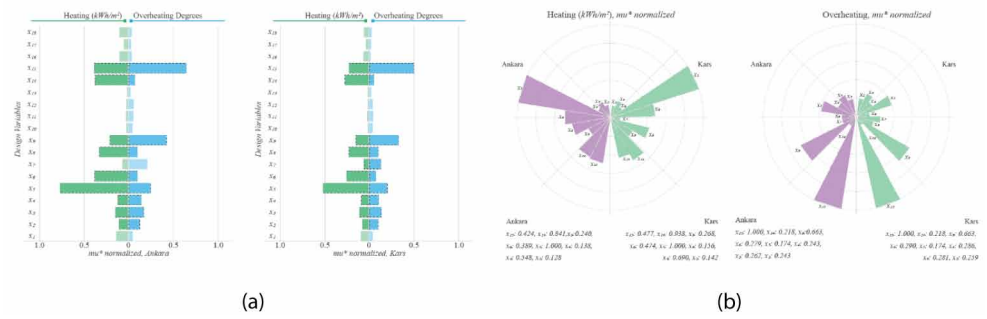

indoor temperature by sunlight radiation. x_5, x_6 are envelope-related design variables, and they are responsible for maintaining indoor heat temperature at a constant level. x_{14} is also in this category.

Respectively, x_1, x_7, x_8, x_{10}, x_{11}, x_{13}, x_{16}, x_{17}, x_{18} were the least essential variables that were fixed. Horizontal and inner shading and north *wwr* variables were also related to sunlight. However, these variables did not cause any significance for the performance outputs. The internal gain variables are essential for the residential units' energy demand because of the indirect interaction with daily occupant activities, yet these variables were not as influential as other design variables. Envelope-related construction variables *u*-value floor and *u*-value wall were not similarly effective for both outputs. x_7 was influential for cooling demand; however, not the equivalent influence ratio for heating demand.

On the contrary, x_8 was effective for heating demand and ineffective for cooling demand. The natural ventilation-related design variables x_{16}, which is the glazing opening fraction, strongly relate to heating demand and, it has resulted in ineffective cooling demand. Hence, these design variables could not transfer to the second step.

Ankara and Kars' sensitivity analysis resulted in similar design variables, i.e., nine design variables for Ankara and ten design variables for Kars. x_2, x_3, x_4, x_5, x_6, x_8, x_9, x_{14}, x_{15} were effective for the variance of the model's two dependent variables, i.e., heating and overheating degrees. Additionally, x_7 was effective for the Kars region, unlike Ankara. Kars has a colder climate comparing to Ankara. **Figure 8** shows that Ankara's effect values result in higher heating demand and overheating degrees. x_2, x_3, x_4, x_9, x_{15} design variables interact with sunlight and have a similar impact on two outputs. However, envelope-related construction design variables were more effective for heating demand as two regions are heating dominant cities, i.e., x_5, x_6, x_8, x_{14} for Ankara, and x_5, x_6, x_7, x_8, x_{14} for Kars. In general, the indoor comfort temperature has a direct relationship with the envelope quality, and as the *u*-values of the construction decreases, the overheating degrees are increasing. Even, Ankara and Kars have very cold climates (e.g., *ASHRAE 5B* and *ASHRAE 7*), the overheating degrees were not much as expected. In parallel, internal gain-related design variables also were evaluated as ineffective for both overheating degrees and heating demand, i.e., x_{17}, x_{18}. All shading variables, x_{10}, x_{11}, x_{12}, and x_{13}, resulted in ineffective due to the low level of sunlight hours for two regions. Lastly, the glazing opening fraction design variable (x_{16}) could not be effective as expected because of the outdoor temperature constraint and lower outdoor temperature values (**Table 2**).

The Variance-Based Sobol Global Sensitivity Analysis

The *Sobol* sensitivity analysis provides variance-based global observation by decomposing the output variance. The analysis accounts for the individual impact (S_1) and total impact (S_T) variables for the model's output. The total effect index represents the first-order effect and all higher-order effects due to the total effect of design variables. In the first phase of *Morris* sensitivity analysis, ten design variables were eliminated for Istanbul and Izmir. Then, eight independent variables were introduced to *GSA*. The analogous design variables were resulted as the most effective for the second phase because of the similar climate properties, e.g., warm-humid. For each analysis, 21999 simulations have been executed based on 1000 iterations. **Figure 9** is the vertical bar chart for the first-order and total effect results of the most effective design variables for Istanbul (a) and Izmir (b). Two performance outputs were presented in the chart for S_1 and S_T indices, i.e., red color tones for heating (kWh/m^2-*year*) and blue color tones for cooling demand (kWh/m^2-*year*).

x_5, x_6, x_9, x_{14}, x_{15} variables were more effective than other variables in S_1 and S_T indices. Except for the impact value of x_3, all these variables were highly effective for the first step of *Morris*'s analysis. Between these variables, x_5, x_6, x_{14} were helpful in heating demand. x_9 and x_{15} were effective for the cooling demand. Despite x_5, x_6, x_{15} are envelope-related variables, and they influence the heating demand, x_9 controls the height of the context buildings, and x_{14} is the solar heat gain coefficient of the window construction. Both are directly related to indoor heating by solar radiation. Therefore, these variables had an impact on cooling demand.

Figure 9. (a) Sobol, Vertical Bar Plot for Istanbul; (b) Sobol, Vertical Bar Plot for Izmir

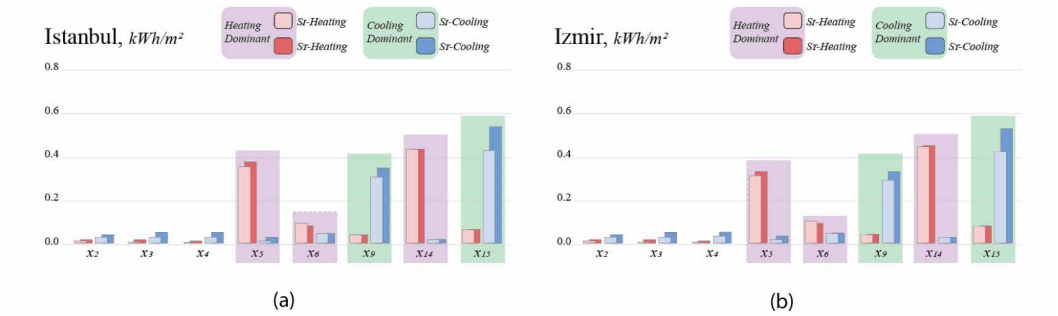

Figure 10 represents the office units' *Sobol* results for Ankara and Kars. The performance outputs for the office unit were different from the residential unit. The cooling demand is unnecessary for Ankara (*ASHRAE climate zone 5B*) and Erzurum (*ASHRAE climate zone 7*). Hence, the heating demand and annual overheating degrees calculation were selected as two outputs of these models. For Ankara, nine variables were influential for the output variance. For Kars, the number of influential design variables was ten. The climate of the Kars is much colder than in Ankara. Therefore, the heating demand is more critical for the region. Even though heating demand-related variables were more dominantly from other variables for Kars, the number of the most influential design variables was identical, i.e., x_5, x_6, x_8, x_9, x_{14}, x_{15}. Like the Izmir and Istanbul analyzes, x_5, x_6, x_8, x_{14} had more influence on the heating demand than envelope-related variables. x_9 and x_{15} had more impact on overheating degrees for both regions. These are solar radiation-related variables for indoor temperature.

The Variance-Based Second-Order Interaction

The *Sobol* sensitivity analysis is a global sensitivity analysis that can quantify first-order and higher-order calculations for input variables. The design variables' individual and total effect were demonstrated for four different climate regions in previous chapters. In this chapter, the second-order effect of the design variables was explained with a correlation matrix for only the Izmir region as an example representation of the methodology (**Figure 11**). Second-order is an index that presents the quantified value of the interactions between design variables. It is different from the total effect because the total effect is the combination of individual impact and the higher-order factors.

In **Figure 11**, interaction values between design variables were demonstrated with color-coding and scalar values. The first graph shows the interactions between design variables according to the heating requirement. The highest interaction between design variables occurred between x_5 - x_3, x_5 - x_4, and x_{15} - x_2. Although there was an interaction between the rest of the design variables, it remained

Figure 10. (a) Sobol, Vertical Bar Plot for Ankara; (b) Sobol, Vertical Bar Plot for Kars

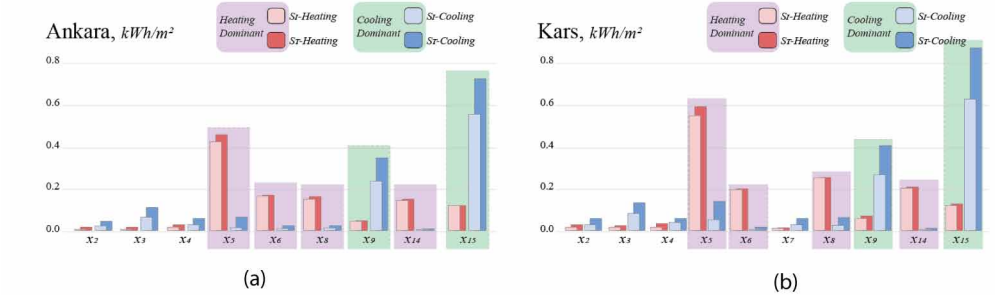

Figure 11. Correlation Matrices for the Interaction of Most Effective Design Variable, (a) Based on Heating Demand, (b) Based on Cooling Demand

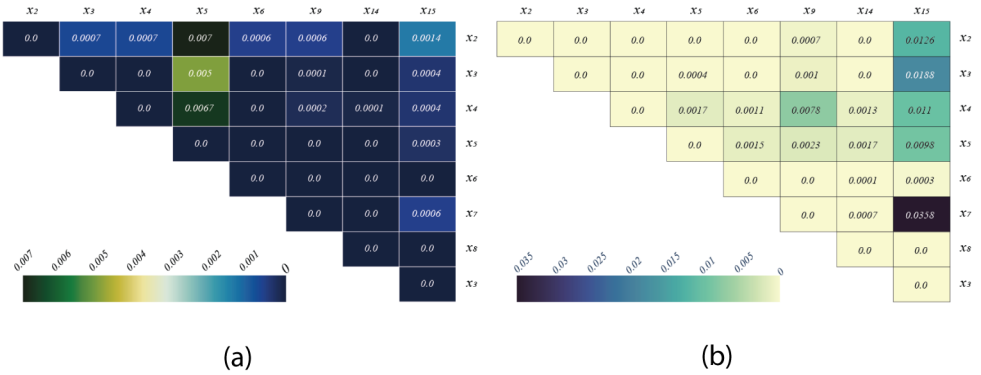

(a) (b)

at meager rates. The second graph is a correlation matrix showing the interaction between design variables according to the cooling demand. According to the results, there is a strong interaction between x_{15} - x_7, x_9 - x_4, x_{15} - x_3, x_{15} - x_2, x_{15} - x_5. Design variables have been in a more active interaction in design cooling demand compared to heating. In particular, the x_{15} design variable is the variable that interacts the most with other design variables.

Design Variable Range Filtering With Factor Mapping

In this chapter, the effective range values were presented for the yearly weighted sum of heating and cooling demand for Istanbul and Izmir and the annual normalized weighted sum of heating demand and overheating degrees for Ankara and Kars. The filtering process was applied to drive the valuable ranges of influential design variables by extracting the 100 most effective results.

Figure 12 points out the distribution results of factor mapping in Istanbul and Izmir. Eight uniformly distributed design variables got some valuable ranges based on the lowest energy demand for two regions. The heating demand values are between 67.50 to 112.80 for Istanbul, and the cooling demand values are 29.04 to 71.03 for Istanbul. Heating energy demand values are between 53.40 to 95.40 (kWh/m^2-$year$) and 44.81 to 82.29 for cooling demand in Izmir. As Izmir higher outdoor temperature and humidity values, the heating demand range is lower, but the cooling demand range is higher than Istanbul simulation results. The x_5 and x_{14} design variables were valued in a narrower

Figure 12. (a) Design Variables Distribution of Istanbul for Range Filtering; (b) Izmir

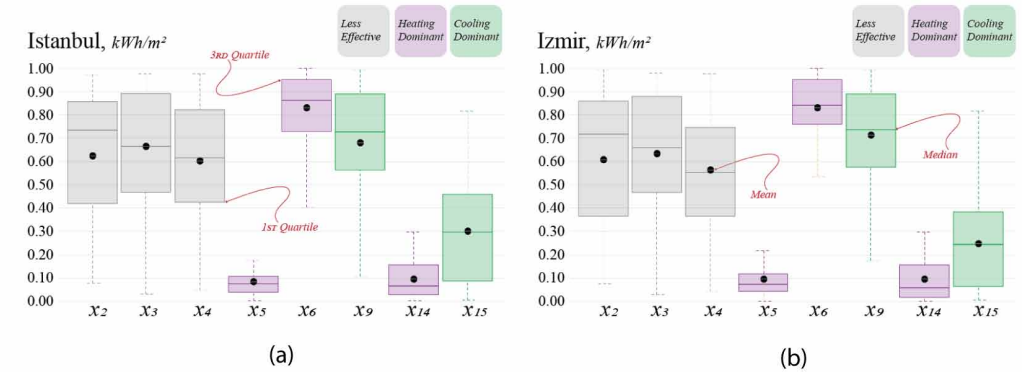

(a) (b)

range compared to other variables. Besides, x_2, x_3, x_4, x_9, and x_{15} obtained the best heating need results by taking values in more comprehensive ranges.

Figure 13 presents the most effective design variable distributions of Ankara and Erzurum for the first 100 best results. Nine for Ankara and ten for Kars uniformly distributed design variables got some valuable range based on the lowest energy demand. The heating demand values are between 34.10 to 61.70 (*kWh/m²-year*), and the overheating degrees are 2854.40 to 18081.80 for Ankara. Heating demand values are between 88.70 to 135.70 (*kWh/m²-year*) and 454.90 to 10408.00 for overheating degrees in Kars. The range of heating demand is higher for Kars because of the annual lower outdoor temperature values. The range of overheating degrees is lower than in Ankara simulations. For both regions, x_5, x_6, and x_{14} were valued in a narrower range, while other variables' variance was higher in a scalar comparison.

Depicting the results of energy analysis with multiple variables is crucial to the more straightforward interpretation of the complicated relations among design variables and performance outputs. For instance, designers have the possibility to sort performance results according to the units' energy performance and which variable corresponds to the selected output value. It is effective for evaluating the design alternatives. Hence, a *PCP* was used to demonstrate global design space. Each data dimension corresponds to a vertical axis on the plot, and each data element is displayed as a series of connected polylines along the dimensions. The vertical axes classify the values from worse to best. As the *PCP*'s shortcoming is when design alternatives are concentrated in very data density, the plot space can become extremely cluttered. Thus, the interactive *brushing* technique can be used to edit values that are important to the designer at the specified point of the design, and the complexity can be reduced. The result of the *brushing* highlights a selected line or collection of lines to isolate parts of the drawing that the designer is interested in when filtering out noise or a dense data set.

Figure 14 demonstrates the most valuable ranges of the most effective eight design variables for Izmir, i.e., heating (Y_1) and cooling energy demand (Y_2) in Izmir. The hundred best design alternatives are the result of the factor mapping. In this representation, the brushing was applied for the lowest heating demand performances. All the design variables data distribution could be presented with the horizontal bar charts on the vertical axes. Therefore, while the users can interactively select the design variable alterations with respect to performance outputs, they can comprehend where the data-dense or short. This representation contributes extra knowledge to the decision-making process.

Figure 15 shows the brushing implication on the heating demand from the hundred best design results representation for Istanbul (a) and Izmir (b). The brushing technique can be applied to multiple design alternatives and outputs simultaneously with *PCP*. In this step, the brushing method was used for the lowest heating demand for two regions to observe the climate effect. With this technique, a minimum of 3 values was reached. Despite the high rate of differentiation in output performance

Figure 13. (a) Design Variables Distribution of Ankara for Range Filtering; (b) Kars

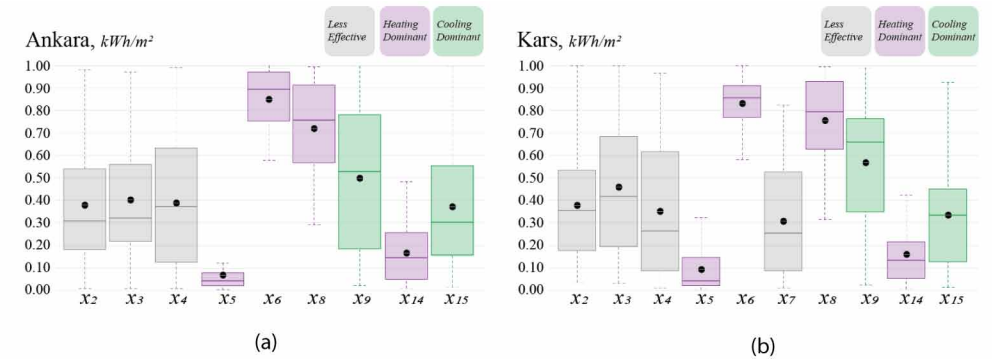

Figure 14. PCP representation of Factor Mapping Results of Izmir

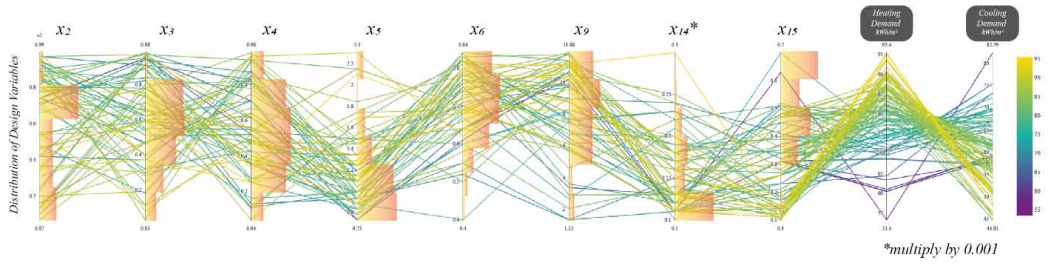

Figure 15. (a) Brushing on PCP for Izmir; (b) Istanbul

(a)

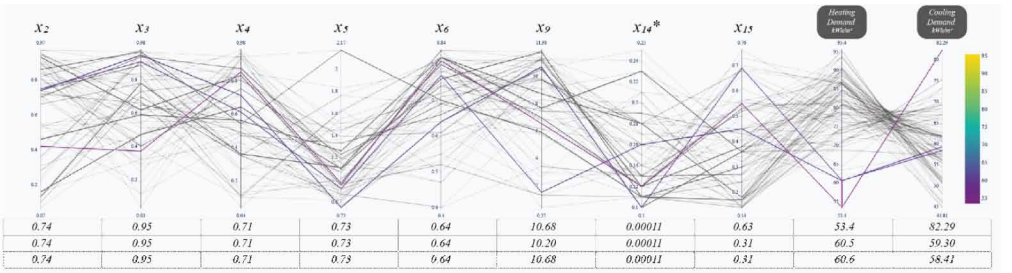

0.74	0.95	0.71	0.73	0.64	10.68	0.00011	0.63	53.4	82.29
0.74	0.95	0.71	0.73	0.64	10.20	0.00011	0.31	60.5	59.30
0.74	0.95	0.71	0.73	0.64	10.68	0.00011	0.31	60.6	58.41

(b)

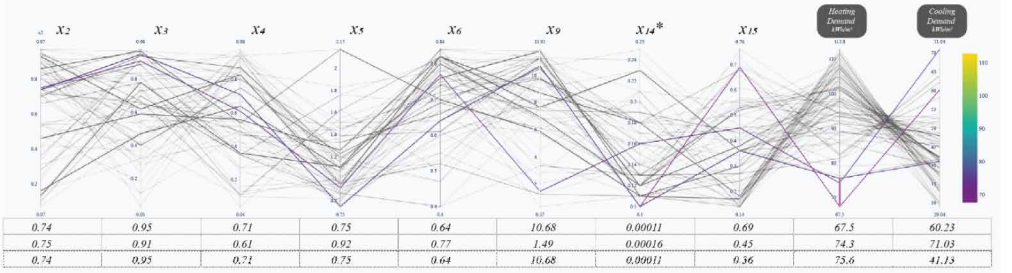

0.74	0.95	0.71	0.75	0.64	10.68	0.00011	0.69	67.5	60.23
0.75	0.91	0.61	0.92	0.77	1.49	0.00016	0.45	74.3	71.03
0.74	0.95	0.71	0.75	0.64	10.68	0.00011	0.36	75.6	41.13

between Istanbul and Izmir, there is a high similarity in design alternatives' values. These comparison values are shown below the *PCP* plots. As a result, the heating demand results were higher, and the cooling demand results lower for Istanbul.

Figure 16 shows *PCP* representation for the hundred best design alternative results for Ankara (a) and Kars (b). Similarly, the brushing technique was applied to the heating demand by achieving a minimum of three values. There is a high rate of differentiations for performance output results and the design variables' assigned values for Ankara and Kars. According to the values under the *PCP* charts, Ankara's minimum value has resulted in 34.1 (kWh/m^2) and 18081 overheating degrees, 88.70 (kWh/m^2) and 10408 for Kars.

CONCLUSION

Early architectural design involves an intense decision-making process for determining the design variables, and the decisions significantly affect the building performance. Thus, it is necessary to analyze the effect of design variables on performance outputs. This article proposes a technique for analyzing the individual and total impacts of design variables, which are determined in early architectural design, on building performance outputs using statistical sensitivity analysis with two

Figure 16. (a) Brushing on PCP for Ankara; (b) Kars

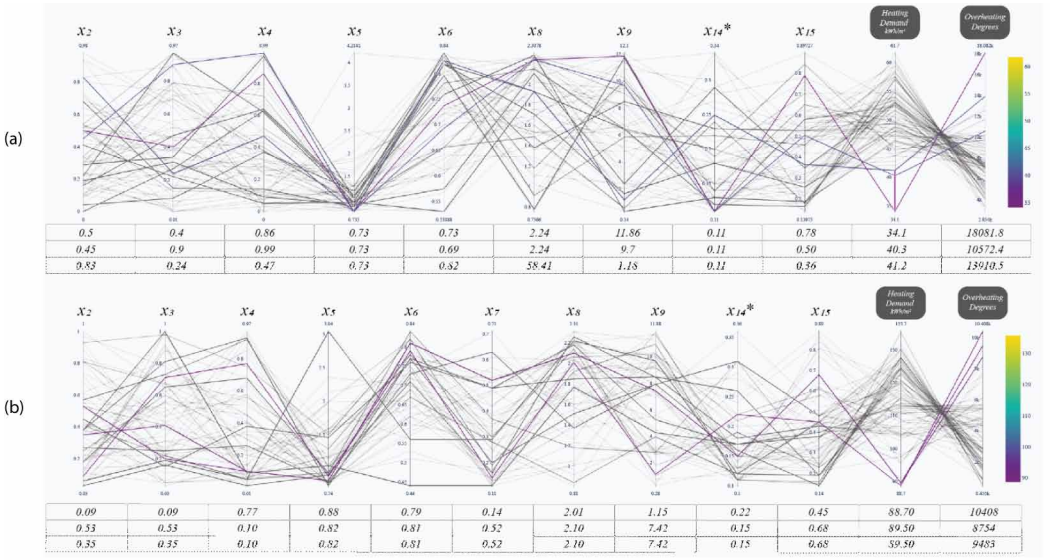

different types of building functions in two different climates. The proposed methodology combines the two-phase sensitivity analysis and three stages involving statistical filtering and visualization. In the first stage, the local sensitivity analysis *Morris* and ineffective design variables were fixed, and in the second stage, the total effect of the design variables on the performance output was measured with the global sensitivity analysis *Sobol*. Four different groups of design variables are used, i.e., heat transfer by conduction, solar gain, ventilation rate, and internal gains.

The number of design variables and their impact rates were different for each case type. The building function was different for two sets of simulations and the sensitivity analysis process. It is not possible to compare two building functions properly. The occupant schedules, the daily activities, equipment load, differs between the two building functions. However, the physical and thermal building parameters and design variables were identical for the two case studies. Therefore, a limited comparison is possible. The residential building simulations were realized in warmer climates, and results presented that design variables have a lower impact on the heating demand than the model's output. Fewer variables were effective for both Istanbul and Izmir, x_2, x_3, x_4, x_5, x_6, x_9, x_{14}, and x_{15}. On the other hand, this number was nine for Ankara (including x_8, *u*-value of the wall) and ten for Kars (including x_8: *u*-value of the wall, and x_7: *u*-value of the floor). Similarly, x_5, x_6, and x_{14} were effective for heating demand and, x_9, x_{15} influenced the cooling demand for residential units and overheating degrees for office units. The most effective design variables' individual effect was shown using factor mapping and the *Parallel Coordinate Graph*. According to the results of the analysis, the effects of design variables occurred in a similar way in the examinations of the residential unit. On the other hand, both the number of design alternatives and their effect on performance output differed for office units. The proposed methodology measured the design variables' individual and interaction impact and showed them interactively for different alternative choices. In line with the proposed methodology, designers can directly observe design variables' effects and determine design combinations in the early architectural design process. In this way, they can apply the performance-based design approach more effectively in the early architectural design process.

FUNDING AGENCY

This research received no specific grant from any funding agency in the public, commercial, or not-for-profit sectors.

REFERENCES

Alam, F. M., McNaught, K. R., & Ringrose, T. J. (2004). Using Morris' randomized OAT design as a factor screening method for developing simulation metamodels. *Proceedings of the 36th Conference on Winter Simulation*, 949–957. doi:10.1109/WSC.2004.1371413

ASHRAE. (2004). *ASHRAE Standard 55-2004 -- Thermal Comfort* (Vol. 2004). 10.1007/s11926-011-0203-9

ASHRAE. (2009). *ASHRAE climatic design conditions 2009/2013/2017*. Retrieved February 4, 2020, from http://ashrae-meteo.info/

ASHRAE. (2013a). ANSI/ASHRAE Standard 62.1-2010. Ventilation for acceptable indoor air quality. Author.

ASHRAE. (2013b). *ASHRAE Standard 90.1-2013 -- Energy Standard For Buildings Except Low-rise Residential Buildings*. Author

Attia, S., Gratia, E., De Herde, A., & Hensen, J. L. M. (2012). Simulation-based decision support tool for early stages of zero-energy building design. *Energy and Building*, *49*, 2–15. doi:10.1016/j.enbuild.2012.01.028

Burhenne, S., Jacob, D., & Henze, G. P. (2011). Sampling based on Sobol'sequences for Monte Carlo techniques applied to building simulations. *Proc. Int. Conf. Build. Simulat*, 1816–1823.

CIBSE. (2006). *Guide A*. Environmental Design.

De Wit, S., & Augenbroe, G. (2002). Analysis of uncertainty in building design evaluations and its implications. *Energy and Building*, *34*(9), 951–958. doi:10.1016/S0378-7788(02)00070-1

Depecker, P., Menezo, C., Virgone, J., & Lepers, S. (2001). Design of buildings shape and energetic consumption. *Building and Environment*, *36*(5), 627–635. doi:10.1016/S0360-1323(00)00044-5

Firth, S. K., Lomas, K. J., & Wright, A. J. (2010). Targeting household energy-efficiency measures using sensitivity analysis. *Building Research and Information*, *38*(1), 25–41. doi:10.1080/09613210903236706

Granadeiro, V., Duarte, J. P., Correia, J. R., & Leal, V. M. S. (2013). Building envelope shape design in early stages of the design process: Integrating architectural design systems and energy simulation. *Automation in Construction*, *32*(September), 196–209. doi:10.1016/j.autcon.2012.12.003

Haarhoff, J., & Mathews, E. H. (2006). A Monte Carlo method for thermal building simulation. *Energy and Building*, *38*(12), 1395–1399. doi:10.1016/j.enbuild.2006.01.009

Hemsath, T. L., & Alagheband Bandhosseini, K. (2015). Sensitivity analysis evaluating basic building geometry's effect on energy use. *Renewable Energy*, *76*, 526–538. doi:10.1016/j.renene.2014.11.044

Herman, J., & Usher, W. (2017). *SALib Documentation*. Release.

Hien, W. N., Poh, L. K., & Feriadi, H. (2000). The use of performance-based simulation tools for building design and evaluation: A Singapore perspective. *Building and Environment*, *35*(8), 709–736. doi:10.1016/S0360-1323(99)00059-1

Iooss, B., & Lemaître, P. (2015). A review on global sensitivity analysis methods. *Uncertainty Management in Simulation-Optimization of Complex Systems*, 101–122.

Kampf, J. H., & Robinson, D. (2010). Optimisation of building form for solar energy utilisation using constrained evolutionary algorithms. *Energy and Building*, *42*(6), 807–814. doi:10.1016/j.enbuild.2009.11.019

Kanters, J., & Horvat, M. (2012). The design process known as IDP: A discussion. *Energy Procedia*, *30*, 1153–1162. doi:10.1016/j.egypro.2012.11.128

Konis, K., Gamas, A., & Kensek, K. (2016). Passive performance and building form: An optimization framework for early-stage design support. *Solar Energy*, *125*, 161–179. doi:10.1016/j.solener.2015.12.020

Kristensen, M. H., & Petersen, S. (2016). Choosing the appropriate sensitivity analysis method for building energy model-based investigations. *Energy and Building*, *130*, 166–176. doi:10.1016/j.enbuild.2016.08.038

LBNL. (2009). Input Output Reference. EnergyPlus.

Macdonald, I. A. (2002). *Quantifying the effects of uncertainty in building simulation*. Academic Press.

Menberg, K., Heo, Y., & Choudhary, R. (2016). Sensitivity analysis methods for building energy models: Comparing computational costs and extractable information. *Energy and Building*, *133*, 433–445. doi:10.1016/j.enbuild.2016.10.005

Morbitzer, C. A. (2003). *Towards the Integration of Simulation into the Building Design Process*. University of Strathclyde.

Mumovic, D. (2009). *A Handbook of Sustainable Building Design and Engineering: An Integrated Approach to Energy, Health and Operational Performance*. Academic Press.

O'Neill, Z., & Niu, F. (2017). Uncertainty and sensitivity analysis of spatio-temporal occupant behaviors on residential building energy usage utilizing Karhunen-Loève expansion. *Building and Environment*, *115*, 157–172. doi:10.1016/j.buildenv.2017.01.025

Østergård, T., Jensen, R. L., & Maagaard, S. E. (2017). Early Building Design: Informed decision-making by exploring multidimensional design space using sensitivity analysis. *Energy and Building*, *142*, 8–22. doi:10.1016/j.enbuild.2017.02.059

Østergård, T., Maagaard, S. E., & Jensen, R. L. (2015). A stochastic and holistic method to support decision-making in early building design. *Proceedings of Building Simulation*, 1885–1892.

Philip, S., Tran, T., & Tanjuatco, L. (2011). eppy: scripting language for E+. *EnergyPlus (Version 0.46)* [Software-GNU AFFERO GENERAL PUBLIC LICENSE]. Available From Https://Pypi. Python. Org/Pypi/Eppy/0.46

Python Software Foundation. (2020). *Batch-processor · PyPI*. Retrieved December 6, 2020, from https://pypi.org/project/batch-processor/

Rasouli, M., Ge, G., Simonson, C. J., & Besant, R. W. (2013). Uncertainties in energy and economic performance of HVAC systems and energy recovery ventilators due to uncertainties in building and HVAC parameters. *Applied Thermal Engineering*, *50*(1), 732–742. doi:10.1016/j.applthermaleng.2012.08.021

Reference, T., & Calculations, E. (2015). *EnergyPlus TM Documentation Engineering Reference. The Reference to EnergyPlus Calculations*.

Roudsari, M. S., & Pak, M. (2013). Ladybug: A parametric environmental plugin for grasshopper to help designers create an environmentally-conscious design. *Proceedings of BS 2013: 13th Conference of the International Building Performance Simulation Association*, 3128–3135.

Ruiz Flores, R., Bertagnolio, S., Lemort, V., Ruiz, R., Bertagnolio, S., & Lemort, V. (2012). Global Sensitivity Analysis applied to Total Energy Use in Buildings. *High Performance Buildings*, 1–10. Retrieved from http://docs.lib.purdue.edu/ihpbc%5Cnhttp://docs.lib.purdue.edu/ihpbc/78%5Cnhttp://orbi.ulg.ac.be/handle/2268/129192

Saltelli, A., Ratto, M., Andres, T., Campolongo, F., Cariboni, J., Gatelli, D., & Tarantola, S. et al. (2007). Global Sensitivity Analysis. The Primer. In *Global Sensitivity Analysis*. The Primer. doi:10.1002/9780470725184

Sobol, I. M. (2001). Global sensitivity indices for non-linear mathematical models and their Monte Carlo estimates. *Mathematics and Computers in Simulation*, *55*(1–3), 271–280. doi:10.1016/S0378-4754(00)00270-6

Struck, C., de Wilde, P. J. C. J., Hopfe, C. J., & Hensen, J. L. M. (2009). An investigation of the option space in conceptual building design for advanced building simulation. *Advanced Engineering Informatics*, *23*(4), 386–395. doi:10.1016/j.aei.2009.06.004

Sun, Y. (2015). Sensitivity analysis of macro-parameters in the system design of net zero energy building. *Energy and Building*, *86*, 464–477. doi:10.1016/j.enbuild.2014.10.031

Topcu, Y. I., & Ulengin, F. (2004). Energy for the future: An integrated decision aid for the case of Turkey. *Energy*, *29*(1), 137–154. doi:10.1016/S0360-5442(03)00160-9

Torben Østergård, R. L. J. (2017). Interactive Building Design Space Exploration Using Regionalized Sensitivity Analysis. *Building Simulation*.

Unzeta, B. B. (2010). *An Urban Weather Generator Coupling a Building Simulation Program with an Urban Canopy Model*. Massachusetts Institute of Technology.

Wang, W., Zmeureanu, R., & Rivard, H. (2005). Applying multi-objective genetic algorithms in green building design optimization. *Building and Environment*, *40*(11), 1512–1525. doi:10.1016/j.buildenv.2004.11.017

Waqas, A., Melati, D., & Melloni, A. (2017). Stochastic simulation and sensitivity analysis of photonic circuit through morris and sobol method. In *Optical Fiber Communication Conference*. Optical Society of America. doi:10.1364/OFC.2017.Th2A.3

Winkelmann, . (2000). EnergyPlus: Energy Simulation Program. *ASHRAE Journal*, *42*, 49–56.

Yang, S., Tian, W., Cubi, E., Meng, Q., Liu, Y., & Wei, L. (2016). Comparison of Sensitivity Analysis Methods in Building Energy Assessment. *Procedia Engineering*, *146*, 174–181. doi:10.1016/j.proeng.2016.06.369

Yildiz, I., & Sosaoglu, B. (2007). Spatial distributions of heating, cooling, and industrial degree-days in Turkey. *Theoretical and Applied Climatology*, *90*(3–4), 249–261. doi:10.1007/s00704-006-0281-1

Yildiz, Y., Korkmaz, K., Göksal Özbalta, T., & Durmus Arsan, Z. (2012). An approach for developing sensitive design parameter guidelines to reduce the energy requirements of low-rise apartment buildings. *Applied Energy*, *93*, 337–347. doi:10.1016/j.apenergy.2011.12.048

Orçun Koral Işeri graduated from Yaşar University, Architecture Department at 2016 and then, he completed his graduate program in the same university in 2018. He specializes in indoor daylight comfort and energy planning in computational design and preliminary architectural design. He does Ph.D. at Middle East Technical University.

Onur Dursun has joined the Department of Built Environment as Senior Lecturer in Quantity Surveying in 2019. Prior to this appointment, he was an Assistant Professor at the Department of Architecture, Yasar University (Izmir, Turkey); a Visiting Lecturer at German University in Cairo (Berlin, Germany); and a Researcher at the Institute of Construction Economics, University of Stuttgart (Germany) and Teaching Assistant at Istanbul Technical University (Turkey). He was awarded a Doctor of Engineering (Dr.-Ing.) degree in the subject of Construction Economics by University of Stuttgart in 2013. He obtained two MSc degrees in Construction Project Management from University of Reading (UK) and Istanbul Technical University (Turkey) in 2008 and 2009, respectively. Dr. Dursun is interested in research areas/topics related to (1) construction economics – early estimation of key project determinants using statistical modelling and machine learning methods; (2) optimization of building design based on selected performance metrics using simulations coupled with genetic algorithms; (3) integration of virtual reality in building design education. Throughout his career, Dr. Dursun has taught wide spectrum of subjects in built environment at all levels - including, but not limited to, construction project management, economic evaluation of building projects, legal aspects of building projects, virtual environments in building design, research approaches and design, and structural design and analysis.